

# Low-threshold topological nanolasers based on second-order corner state

Weixuan Zhang,<sup>1,2,\*</sup> Xin Xie,<sup>3,4,\*</sup> Huiming Hao,<sup>5</sup> Jianchen Dang,<sup>3,4</sup>  
Shan Xiao,<sup>3,4</sup> Shushu Shi,<sup>3,4</sup> Haiqiao Ni,<sup>5</sup> Zhichuan Niu,<sup>5,†</sup> Can  
Wang,<sup>3,4,6</sup> Kuijuan Jin,<sup>3,4,6</sup> Xiangdong Zhang,<sup>1,2,‡</sup> and Xiulai Xu<sup>3,4,6,§</sup>

<sup>1</sup>*Key Laboratory of advanced optoelectronic quantum architecture  
and measurements of Ministry of Education, School of Physics,  
Beijing Institute of Technology, 100081, Beijing, China*

<sup>2</sup>*Beijing Key Laboratory of Nanophotonics & Ultrafine Optoelectronic Systems,  
Micro-nano Center, School of Physics,  
Beijing Institute of Technology, 100081, Beijing, China*

<sup>3</sup>*Beijing National Laboratory for Condensed Matter Physics,  
Institute of Physics, Chinese Academy of Sciences, Beijing 100190, China*

<sup>4</sup>*CAS Center for Excellence in Topological Quantum  
Computation and School of Physical Sciences,  
University of Chinese Academy of Sciences, Beijing 100049, China*

<sup>5</sup>*State Key Laboratory of Superlattices and Microstructures,  
Institute of Semiconductors Chinese Academy of Sciences, Beijing 100083, China*

<sup>6</sup>*Songshan Lake Materials Laboratory,  
Dongguan, Guangdong 523808, China*

## Abstract

The topological lasers, which are immune to imperfections and disorders, have been recently demonstrated based on many kinds of robust edge states, being mostly at microscale. The realization of 2D on-chip topological nanolasers, having the small footprint, low threshold and high energy efficiency, is still to be explored. Here, we report on the first experimental demonstration of the topological nanolaser with high performance in 2D photonic crystal slab. Based on the generalized 2D Su-Schrieffer-Heeger model, a topological nanocavity is formed with the help of the Wannier-type 0D corner state. Laser behaviors with high performance including low threshold and high spontaneous emission coupling factor are observed with quantum dots as the active material. In particular, the observed lowest threshold is about  $1 \mu W$  and the highest spontaneous emission coupling factor can reach to 0.81. Such performance is much better than that of topological edge lasers and comparable to conventional photonic crystal nanolasers. Our experimental demonstration of the low-threshold topological nanolaser will be of great significance to the development of topological nanophotonic circuitry for manipulation of photons in classical and quantum regimes.

The investigation of topological photonics has become one of the most fascinating frontiers in recent years [1–14]. In addition to the conventional passive and linear system, exploring the topological phenomena in highly nonlinear environments also possesses significant influences [15–24]. Recently, the concept of topological lasers, whose lasing mode exhibits topologically protected transportation with the help of robust 1D edge state in 2D systems, is proposed and demonstrated [15–17]. The pioneer work is the study of lasing on the nonreciprocal topological cavities, which are formed by a closed quantum-Hall like edge state, at telecommunication wavelengths [15]. While, due to the weak magneto-optic effect, the topological band-gap is only about 40 *pm*. The first magnet-free scheme for the realization of single-mode topological lasers is based on an array of ring resonators in 2D, where the notably higher slope efficiencies is observed compared to the trivial counterparts [16, 17]. Besides the utilization of 1D edge state, the 0D boundary states existing in 1D lattices with non-trivial Zak phases [18–21] and the topological bulk state around the band edge [22] have also been used to realize topological lasers. However, the currently designed topological lasing systems are almost at microscale, so that the corresponding thresholds are usually about several milliwatts. The topological nanolasers, combining the advantages of topological robustness and nanolasers including the small footprint, low threshold and high energy efficiency [25–34], are still lacking except for the scheme using 0D interface state in the 1D photonic beam with threshold being about 46  $\mu W$  [21].

Recently, a new class of symmetry-protected higher-order topological insulators, which sustain lower-dimensional boundary states and obey a generalization of the standard bulk-boundary correspondence, have been proposed [35–50]. In 2D cases, the 0D corner state can be usually formed by two mechanisms. One is related to quantized bulk quadrupole polarization [35–39] and the other is derived from the edge dipole polarization quantized by the 2D Zak phase [43–45]. The latter model can be easily implemented in the compact magnet-free optical platform [44] and be used to construct topological nanocavity [45]. The problem is whether we can exploit the topological nanocavity, sustaining the high quality (Q) factor and small mode volume comparable to the conventional photonic crystal nanocavity [51], to realize the topological nanolaser with low threshold and high energy efficiency.

In this work, we report on the first experimental demonstration of the topological nanolaser in 2D topological photonic crystal (PhC) nanocavity, which sustains the Wannier-type 0D corner state at nanoscale. Our designed topological nanocavity is based on the 2D

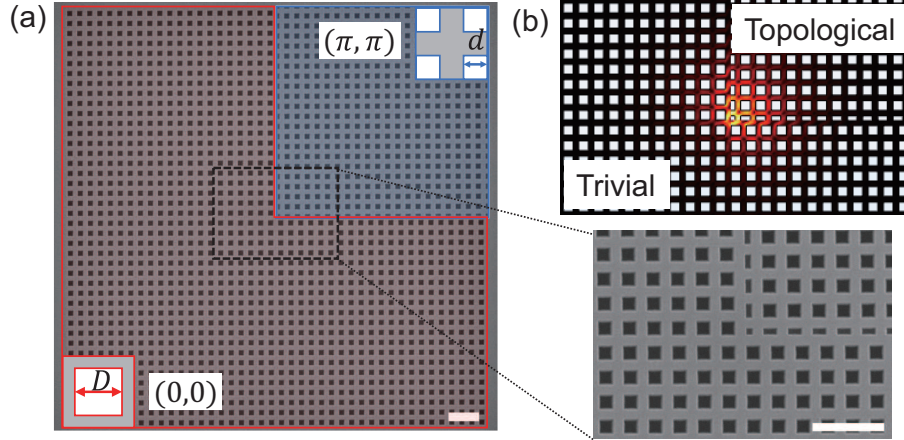


FIG. 1. (a) Scanning electron microscope image of a fabricated 2D topological PhC cavity in a square shape. Inset on the right shows an enlarged image around the corner. The scale bar is  $1 \mu m$ . The topological nanocavity consists of two topologically distinct PhC which are indicated by the red and blue areas. They have different unit cells as shown in insets.  $d$  and  $D$  are the lengths of the squares in blue and red unit cells, in which  $D = 2d$ . (b) Electric field profile of topological corner state calculated by the finite element method [52].

Su-Schrieffer-Heeger (SSH) model, in which the corner state is induced by the edge dipole polarization quantized by the 2D Zak phase. By suitably tuning the gap distance between the trivial and non-trivial parts of the PhC slab, the higher Q factor can be achieved. The robustness of corner state with respect to defects in the bulk of PhC is demonstrated. Lasing behaviors at corner state with high performance including low threshold and high spontaneous emission coupling factor ( $\beta$ ), are observed with InGaAs quantum dots (QDs) serving as active material. The high performance of the topological nanolaser is comparable to the conventional semiconductor nanolasers [25–28], indicating the great prospects of the topological nanocavity for a wide range of applications in the topological nanophotonic circuitry.

Based on the generalized 2D SSH model, a topological nanocavity can be constructed, as shown in Fig. 1(a). It consists of two kinds of PhC in a square shape, which have the same period  $a$  but different unit cells, as indicated by the red and blue areas in Fig. 1(a). These two regions share the common band structure but possess different topologies, which are characterized by the 2D Zak phase  $\theta^{Zak}$ , a quantity defined by the integration of Berry connection within the first Brillouin zone [53, 54]. The PhC in blue (red) area has a nontrivial

(trivial) 2D Zak phase of  $\theta^{Zak} = (\pi, \pi)$  ( $\theta^{Zak} = (0, 0)$ ). In this case, according to the bulk-edge-corner correspondence, the midgap 0D corner state can be induced at the intersection of two boundaries with non-zero edge polarizations, which are protected by the nontrivial 2D Zak phase in the bulk. Furthermore, the eigen-field of this corner state is highly confined at nanoscale as show in Fig. 1(b), which can greatly enhance the light-matter interaction, thus having potential applications such as the construction of topological nanolasers.

To improve the laser performance, the Q factor of corner state is optimized by suitably tuning the gap distance ( $g$ ) between the trivial and non-trivial parts of the PhC slab as shown in the inset of Fig. 2(a). The black and red lines in Fig. 2(a) represent the calculated results of Q factor and resonance wavelength of the corner state with different values of  $g$ . It is clearly shown that the Q factor first increases then decreases with  $g$  gradually going up, meanwhile, the corner state shows a redshift. When  $g = 60$  nm, the corner mode supports a high Q factor of 50,000 and a small mode volume of  $0.61(\lambda/n)^3$ . It is worthy to note that the Q factor and mode volume of corner state are both able to be disturbed by introducing perturbations around the corner. Nevertheless, the corner state always survives even with harsh perturbations on the bulk of PhC as far as the topological band-gap remains opened, which could be a practical advantage for robust applications.

We fabricated the designed topological nanocavity with different parameters into a 160-nm-thick GaAs slab using electron beam lithography followed by inductively coupled plasma and wet etching process. The wet etching with HF solution was used to remove the sacrificial layer to form air bridge. The GaAs slab is grown by molecular beam epitaxy and contains a single layer of InGaAs QDs at the center with a density of about  $500 \mu m^{-2}$ . The scanning electron microscope image of a fabricated cavity is shown in Fig. 1(a), in which the inset on the right shows an enlarged image around the corner.

To optically characterize the corner state, we performed the confocal micro-photoluminescence (PL) measurements at 4.2 K using a liquid helium flow cryostat. An objective lens with a numerical aperture of 0.7 was used to address the sample. It was excited by a continuous laser with wavelength of 532 nm. The PL signal was dispersed by a grating spectrometer and detected with a liquid-nitrogen-cooled charge coupled device camera. Fig. 2(b) shows PL spectra for cavities with different  $g$ , in which the corner states and edge states are indicated. With increasing  $g$  from 20 nm to 50 nm, the corner state exhibits redshift and the corresponding Q factor increases, which are consistent with the numerical results in

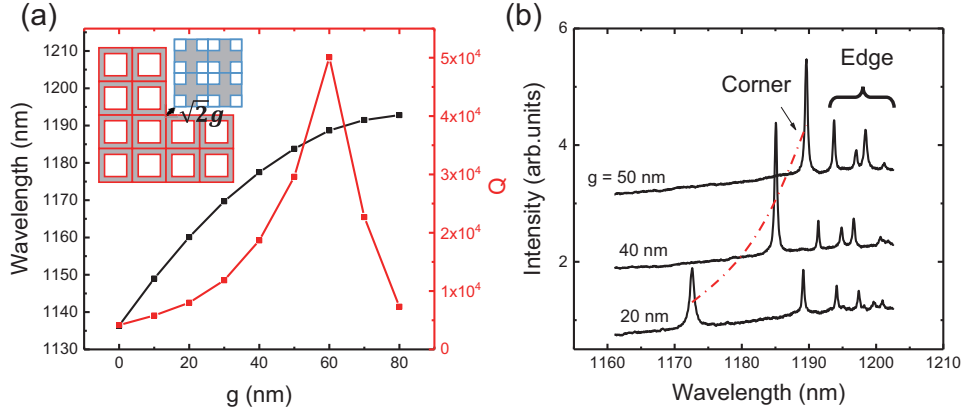


FIG. 2. (a) Calculated Q factors (red) and wavelengths (black) of corner state with different  $g$ . The Q factors and wavelengths are calculated by the finite element method. Other parameters for these cavities are that  $a = 380$  nm,  $D = 242$  nm. Inset shows the schematic of Q optimization, in which the topological PhC is shifted away from the corner by  $\sqrt{2}g$  along the diagonal direction. (b) PL spectra for cavities with  $a = 380$  nm,  $D = 242$  nm and different  $g$ . Red dashed line represents the corner state. These peaks in long-wavelength range originate from edge states. The PL spectra are shifted for clarity.

Fig. 2(a). However, limited by the unavoidable fabrication imperfections, the fabricated Q factors are about an order of magnitude lower than the theoretical prediction, which are usually 2500-5000.

Then, in order to demonstrate the topological protection of the corner state, we fabricated topological cavities without and with defects introduced by missing square holes in bulk of PhC (Inset in Fig. 3(b)). Fig. 3(a) shows the PL spectra for defect-free cavities. In this case, the fluctuation of corner state and edge state is observed, which may result from the fabrication imperfections. In the current state-of-the-art techniques, a fabrication deviation of about 2-5 nm always exists. According to the calculated results (see Supplementary Material), the detuning of resonance wavelength can be up to 6 nm when random deviations about 2-5 nm are introduced around the corner. The observed fluctuation of wavelength about 2 nm is within the range. Additionally, the calculated Q factor with perturbations around corner can be decreased by about an order of magnitude, and that can well explain the deviation of fabricated Q factors from the calculated result.

Although the Q factor and resonance wavelength of corner state are easily to be influenced

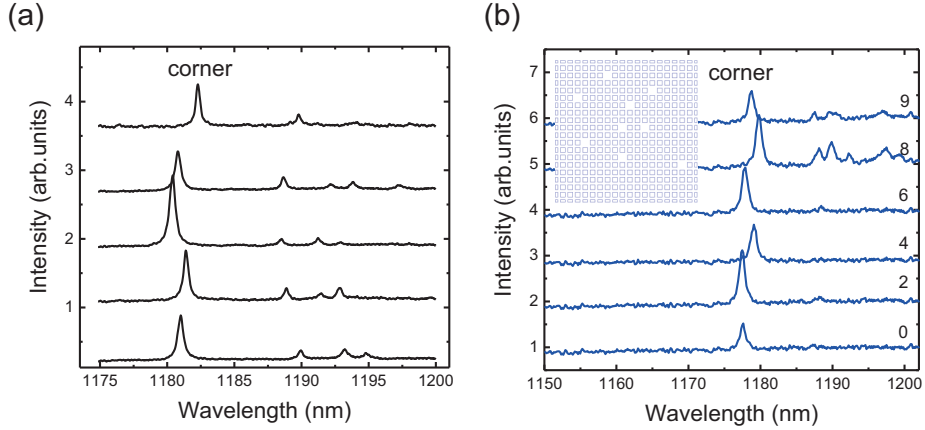


FIG. 3. (a) PL spectra of defect-free cavities with the parameters of  $a = 380$  nm,  $D = 242$  nm and  $g = 50$  nm. (b) PL spectra of cavities with different numbers of defects as shown in inset. The numbers represent the number of missing square holes in bulk of PhC. Here, the missing square holes are several periods away from the corner. The PL spectra are shifted for clarity.

by the disorder around the corner, the corner state always survives even with many defects in the bulk of PhC since it is topologically protected by the nontrivial 2D Zak phases. Fig. 3(b) shows the PL spectra of cavities with different amounts of defects in the bulk of PhC, which are introduced by missing square holes as shown in the inset. The corner state still exists even with nine missing holes except for small fluctuations of Q factors and wavelengths. The wavelength fluctuation is about 2.5 nm, which is comparable to the defect-free samples in Fig. 3(a). According to the numerical results, the wavelength deviation of cavities with 9 missing holes is about 0.8 nm, which can be ignored in comparison with the deviation induced by fabrication imperfection. The fluctuation in cavities with defects thus mainly results from the fabrication imperfections. Therefore, the existence of corner state is robust to the defects in the bulk of PhC, which demonstrates the topological protection of corner state.

To verify the laser behavior of corner state with QDs as gain, we investigate the pump-power dependence of corner state emission in the topological nanocavities. In this case, the continuous laser with wavelength of 532 nm was used to pump QDs. We have measured many cavities and observed the lasing and non-lasing behaviors (see Supplementary Material). Fig. 4 illustrates lasing behaviors with high performance from two cavities, in which (a)-(b) correspond to the results from Cavity a ( $a = 360$  nm,  $D = 222$  nm and  $g = 30$  nm)

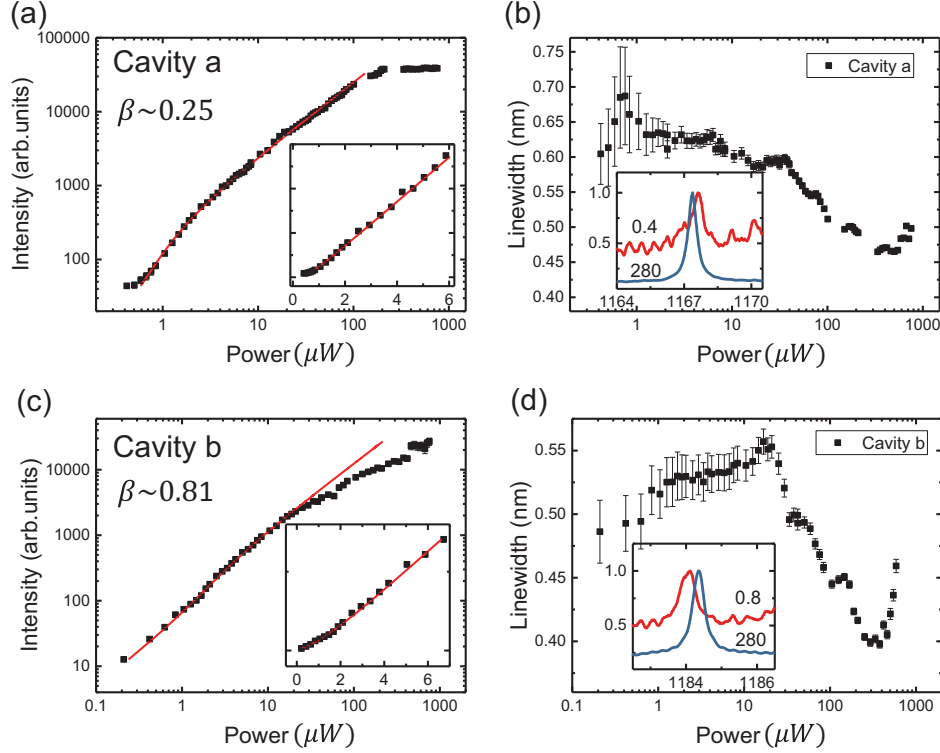


FIG. 4. Pump-power dependence of corner state from (a) Cavity a with  $a = 360$  nm,  $D = 222$  nm and  $g = 30$  nm and (c) Cavity b with  $a = 380$  nm,  $D = 242$  nm and  $g = 50$  nm, which are on a logarithmic scale. Insets show the enlarged curve around threshold on a linear scale. Squares represent the experimental data and the line represents the fitted result by semiconductor laser model.  $\beta$  for Cavity a and b are estimated as about 0.25 and 0.81, respectively. Their lasing thresholds are about  $1 \mu W$  and  $2 \mu W$ . Linewidths of corner state as function of pump power from (b) Cavity a and (d) Cavity b. Insets show the normalized PL spectra with different pump powers. The unit of pump powers is  $\mu W$ . Linewidth shows a clear narrowing. The linewidths and intensities are both extracted by fitting high-resolution spectra with Lorentz peak functions.

and (c)-(d) from Cavity b ( $a = 380$  nm,  $D = 242$  nm and  $g = 50$  nm). The linewidths and intensities of corner state are both extracted by fitting high-resolution spectra with Lorentz peak functions. For Cavity a, the light-in-light-out (L-L) plot on logarithmic scale in Fig. 4(a) shows a mild ‘s’ shape, suggesting a lasing oscillation with high  $\beta$ . A clear kink is observed in the L-L curve on a linear scale, indicating a low threshold about  $1 \mu W$ . The  $\beta$  factor is extracted by fitting the curve with semiconductor laser model [55] (see



Supplementary Material), which is about 0.25. For Cavity b, the L-L curve in Fig. 4(c) exhibits similar behaviors but the ‘s’ shape and kink are not distinct compared with Cavity a, suggesting a higher  $\beta$  about 0.81. The threshold is around  $2 \mu W$ , which is a little larger than that of Cavity a. It may result from smaller absorption efficiency of incident power and larger mode volume for Cavity b. The estimated absorption efficiency for Cavity b is around five times lower than that of Cavity a, which may result from the defect-related optical loss. Meanwhile, the calculated mode volumes for Cavity a and b are  $0.24 (\lambda/n)^3$  and  $0.61 (\lambda/n)^3$ , respectively. In this case, the Cavity b possesses a larger region with high cavity field, which will lead to more QDs coupled with the cavity, corresponding to a greater transparent carrier number  $N_T$ . With increasing  $N_T$ , the threshold will increase, as shown in Supplementary Material. The observed thresholds of our proposed higher-order topological nanolaser are about three orders of magnitude lower than that of the current topological edge lasers [15, 17–20], furthermore are around two percent of the threshold in the topological nanolaser based on 0D interface state [21].

In addition, the measured linewidths for two cavities in Fig. 4(b) and (d) exhibit a clear decline and spectral narrowing in PL are shown in insets, further verifying the laser behaviors in the topological nanocavities. The pronounced linewidth re-broadening around the threshold is observed, which is a signature for lasing in PhC QD nanolaser [28]. It is worthy to note that the saturation of intensities and increase of linewidths at high pump power may result from heating in nanocavities. At pump power about  $0.5 \mu W$  which is below the thresholds, the Q factors for the two cavities are estimated as about 1700 and 2200, respectively. Therefore, the low threshold and high  $\beta$  can be attributed to the small volume and high Q factor which lead to strong optical confinement. The high performance of the topological nanolaser is comparable to that of conventional nanolasers [25–28], indicating the great prospect in applications with built-in protection.

In summary, we demonstrated the topological nanolaser with high performance based on the second-order topological corner state in 2D PhC slabs for the first time. The Q factor of corner state has been optimized by suitably tuning the distance between topologically distinct PhC slabs, which is confirmed both theoretically and experimentally. The topological protection of corner state is demonstrated by introducing defects in the bulk of PhC. The laser behaviors with high performance, including low threshold about  $1 \mu W$  and high  $\beta$  about 0.81, are observed. The observed thresholds are much lower than current topological

lasers due to small mode volume and high Q factor, and the performance is comparable to the conventional nanolasers. Our result shows an example on downscaling the applications of topological photonics into nanoscale and demonstrate the great potential of the topological nanocavity on the applications in topological nanophotonic devices.

This work was supported by the National Natural Science Foundation of China (Grants No. 11934019, No.11721404, No. 51761145104, No. 61675228, and No. 11874419), the National key R&D Program of China (Grant No. 2017YFA0303800 and No. 2018YFA0306101), the Key R&D Program of Guangdong Province (Grant No. 2018B030329001), the Strategic Priority Research Program (Grant No. XDB28000000), the Instrument Developing Project (Grant No. YJKYYQ20180036) and the Interdisciplinary Innovation Team of the Chinese Academy of Sciences.

---

\* Contributed equally to this work.

† zcnium@semi.ac.cn

‡ zhangxd@bit.edu.cn

§ xlxu@iphy.ac.cn

- [1] FDM Haldane and S Raghu, “Possible realization of directional optical waveguides in photonic crystals with broken time-reversal symmetry,” *Phys. Rev. Lett.* **100**, 013904 (2008).
- [2] Ling Lu, John D Joannopoulos, and Marin Soljačić, “Topological photonics,” *Nat. Photonics* **8**, 821 (2014).
- [3] Tomoki Ozawa, Hannah M Price, Alberto Amo, Nathan Goldman, Mohammad Hafezi, Ling Lu, Mikael C Rechtsman, David Schuster, Jonathan Simon, Oded Zilberberg, *et al.*, “Topological photonics,” *Rev. Mod. Phys.* **91**, 015006 (2019).
- [4] Zheng Wang, Yidong Chong, John D Joannopoulos, and Marin Soljačić, “Observation of unidirectional backscattering-immune topological electromagnetic states,” *Nature* **461**, 772 (2009).
- [5] Kejie Fang, Zongfu Yu, and Shanhui Fan, “Realizing effective magnetic field for photons by controlling the phase of dynamic modulation,” *Nat. Photonics* **6**, 782 (2012).
- [6] Mikael C Rechtsman, Julia M Zeuner, Yonatan Plotnik, Yaakov Lumer, Daniel Podolsky, Felix Dreisow, Stefan Nolte, Mordechai Segev, and Alexander Szameit, “Photonic floquet

- topological insulators,” *Nature* **496**, 196 (2013).
- [7] Alexander B Khanikaev, S Hossein Mousavi, Wang-Kong Tse, Mehdi Kargarian, Allan H MacDonald, and Gennady Shvets, “Photonic topological insulators,” *Nat. Mater.* **12**, 233 (2013).
- [8] Mohammad Hafezi, S Mittal, J Fan, A Migdall, and JM Taylor, “Imaging topological edge states in silicon photonics,” *Nat. Photonics* **7**, 1001 (2013).
- [9] Wen-Jie Chen, Shao-Ji Jiang, Xiao-Dong Chen, Baocheng Zhu, Lei Zhou, Jian-Wen Dong, and Che Ting Chan, “Experimental realization of photonic topological insulator in a uniaxial metacrystal waveguide,” *Nat. Commun.* **5**, 5782 (2014).
- [10] Long-Hua Wu and Xiao Hu, “Scheme for achieving a topological photonic crystal by using dielectric material,” *Phys. Rev. Lett.* **114**, 223901 (2015).
- [11] Sabyasachi Barik, Aziz Karasahin, Christopher Flower, Tao Cai, Hirokazu Miyake, Wade DeGottardi, Mohammad Hafezi, and Edo Waks, “A topological quantum optics interface,” *Science* **359**, 666–668 (2018).
- [12] Sunil Mittal, Elizabeth A Goldschmidt, and Mohammad Hafezi, “A topological source of quantum light,” *Nature* **561**, 502 (2018).
- [13] Jean-Luc Tambasco, Giacomo Corrielli, Robert J Chapman, Andrea Crespi, Oded Zilberberg, Roberto Osellame, and Alberto Peruzzo, “Quantum interference of topological states of light,” *Sci.Adv.* **4**, eaat3187 (2018).
- [14] Yao Wang, Yong-Heng Lu, Feng Mei, Jun Gao, Zhan-Ming Li, Hao Tang, Shi-Liang Zhu, Suotang Jia, and Xian-Min Jin, “Direct observation of topology from single-photon dynamics,” *Phys. Rev. Lett.* **122**, 193903 (2019).
- [15] Babak Bahari, Abdoulaye Ndao, Felipe Vallini, Abdelkrim El Amili, Yeshaiahu Fainman, and Boubacar Kanté, “Nonreciprocal lasing in topological cavities of arbitrary geometries,” *Science* **358**, 636–640 (2017).
- [16] Gal Harari, Miguel A Bandres, Yaakov Lumer, Mikael C Rechtsman, Yi Dong Chong, Mercedeh Khajavikhan, Demetrios N Christodoulides, and Mordechai Segev, “Topological insulator laser: theory,” *Science* **359**, eaar4003 (2018).
- [17] Miguel A Bandres, Steffen Wittek, Gal Harari, Midya Parto, Jinhan Ren, Mordechai Segev, Demetrios N Christodoulides, and Mercedeh Khajavikhan, “Topological insulator laser: Experiments,” *Science* **359**, eaar4005 (2018).

- [18] Han Zhao, Pei Miao, Mohammad H Teimourpour, Simon Malzard, Ramy El-Ganainy, Henning Schomerus, and Liang Feng, “Topological hybrid silicon microlasers,” *Nat. Commun.* **9**, 981 (2018).
- [19] Midya Parto, Steffen Wittek, Hossein Hodaei, Gal Harari, Miguel A Bandres, Jinhan Ren, Mikael C Rechtsman, Mordechai Segev, Demetrios N Christodoulides, and Mercedeh Khajavikhan, “Edge-mode lasing in 1d topological active arrays,” *Phys. Rev. Lett.* **120**, 113901 (2018).
- [20] P St-Jean, V Goblot, E Galopin, A Lemaître, T Ozawa, L Le Gratiet, I Sagnes, J Bloch, and A Amo, “Lasing in topological edge states of a one-dimensional lattice,” *Nat. Photonics* **11**, 651 (2017).
- [21] Yasutomo Ota, Ryota Katsumi, Katsuyuki Watanabe, Satoshi Iwamoto, and Yasuhiko Arakawa, “Topological photonic crystal nanocavity laser,” *Commun. Phys.* **1**, 86 (2018).
- [22] Zeng-Kai Shao, Hua-Zhou Chen, Suo Wang, Xin-Rui Mao, Zhen-Qian Yang, Shao-Lei Wang, Xing-Xiang Wang, Xiao Hu, and Ren-Min Ma, “A high-performance topological bulk laser based on band-inversion-induced reflection,” *Nat. Nanotechnol.* **15**, 67–72 (2020).
- [23] Yongquan Zeng, Udvas Chattopadhyay, Bofeng Zhu, Bo Qiang, Jinghao Li, Yuhao Jin, Lianhe Li, Alexander Giles Davies, Edmund Harold Linfield, Baile Zhang, Yidong Chong, and Qi Jie Wang, “Electrically pumped topological laser with valley edge modes,” *Nature* **578**, 246–250 (2020).
- [24] Daria Smirnova, Daniel Leykam, Yidong Chong, and Yuri Kivshar, “Nonlinear topological photonics,” arXiv preprint arXiv:1912.01784 (2019).
- [25] Yasutomo Ota, Masahiro Kakuda, Katsuyuki Watanabe, Satoshi Iwamoto, and Yasuhiko Arakawa, “Thresholdless quantum dot nanolaser,” *Opt. Express* **25**, 19981–19994 (2017).
- [26] Hoon Jang, Indra Karnadi, Putu Pramudita, Jung-Hwan Song, Ki Soo Kim, and Yong-Hee Lee, “Sub-microwatt threshold nanoisland lasers,” *Nat. Commun.* **6**, 8276 (2015).
- [27] Masato Takiguchi, Hideaki Taniyama, Hisashi Sumikura, Muhammad Danang Birowosuto, Eiichi Kuramochi, Akihiko Shinya, Tomonari Sato, Koji Takeda, Shinji Matsuo, and Masaya Notomi, “Systematic study of thresholdless oscillation in high- $\beta$  buried multiple-quantum-well photonic crystal nanocavity lasers,” *Opt. Express* **24**, 3441–3450 (2016).
- [28] Stefan Strauf and Frank Jahnke, “Single quantum dot nanolaser,” *Laser Photonics Rev.* **5**, 607–633 (2011).

- [29] Oskar Painter, RK Lee, Axel Scherer, A Yariv, JD O’Brien, PD Dapkus, and I Kim, “Two-dimensional photonic band-gap defect mode laser,” *Science* **284**, 1819–1821 (1999).
- [30] Hong-Gyu Park, Se-Heon Kim, Soon-Hong Kwon, Young-Gu Ju, Jin-Kyu Yang, Jong-Hwa Baek, Sung-Bock Kim, and Yong-Hee Lee, “Electrically driven single-cell photonic crystal laser,” *Science* **305**, 1444–1447 (2004).
- [31] Philippe Hamel, Samir Haddadi, Fabrice Raineri, Paul Monnier, Gregoire Beaudoin, Isabelle Sagnes, Ariel Levenson, and Alejandro M Yacomotti, “Spontaneous mirror-symmetry breaking in coupled photonic-crystal nanolasers,” *Nat. Photonics* **9**, 311–315 (2015).
- [32] Susumu Noda, Mitsuru Yokoyama, Masahiro Imada, Alongkarn Chutinan, and Masamitsu Mochizuki, “Polarization mode control of two-dimensional photonic crystal laser by unit cell structure design,” *Science* **293**, 1123–1125 (2001).
- [33] Yi Yu, Weiqi Xue, Elizaveta Semenova, Kresten Yvind, and Jesper Mork, “Demonstration of a self-pulsing photonic crystal fano laser,” *Nat. Photonics* **11**, 81 (2017).
- [34] Masahiro Yoshida, Menaka De Zoysa, Kenji Ishizaki, Yoshinori Tanaka, Masato Kawasaki, Ranko Hatsuda, Bongshik Song, John Gellela, and Susumu Noda, “Double-lattice photonic-crystal resonators enabling high-brightness semiconductor lasers with symmetric narrow-divergence beams,” *Nat. Mater.* **18**, 121–128 (2019).
- [35] Wladimir A Benalcazar, B Andrei Bernevig, and Taylor L Hughes, “Quantized electric multipole insulators,” *Science* **357**, 61–66 (2017).
- [36] Stefan Imhof, Christian Berger, Florian Bayer, Johannes Brehm, Laurens W Molenkamp, Tobias Kiessling, Frank Schindler, Ching Hua Lee, Martin Greiter, Titus Neupert, *et al.*, “Topoelectrical-circuit realization of topological corner modes,” *Nat. Phys.* **14**, 925 (2018).
- [37] Christopher W Peterson, Wladimir A Benalcazar, Taylor L Hughes, and Gaurav Bahl, “A quantized microwave quadrupole insulator with topologically protected corner states,” *Nature* **555**, 346 (2018).
- [38] Marc Serra-Garcia, Valerio Peri, Roman Süsstrunk, Osama R Bilal, Tom Larsen, Luis Guillermo Villanueva, and Sebastian D Huber, “Observation of a phononic quadrupole topological insulator,” *Nature* **555**, 342 (2018).
- [39] Sunil Mittal, Venkata Vikram Orre, Guanyu Zhu, Maxim A Gorlach, Alexander Poddubny, and Mohammad Hafezi, “Photonic quadrupole topological phases,” *Nat. Photonics* **13**, 692–696 (2019).

- [40] Josias Langbehn, Yang Peng, Luka Trifunovic, Felix von Oppen, and Piet W Brouwer, “Reflection-symmetric second-order topological insulators and superconductors,” *Phys. Rev. Lett.* **119**, 246401 (2017).
- [41] Motohiko Ezawa, “Higher-order topological insulators and semimetals on the breathing kagome and pyrochlore lattices,” *Phys. Rev. Lett.* **120**, 026801 (2018).
- [42] Frank Schindler, Zhijun Wang, Maia G Vergniory, Ashley M Cook, Anil Murani, Shamashis Sengupta, Alik Yu Kasumov, Richard Deblock, Sangjun Jeon, Ilya Drozdov, *et al.*, “Higher-order topology in bismuth,” *Nat. Phys.* **14**, 918 (2018).
- [43] Bi-Ye Xie, Guang-Xu Su, Hong-Fei Wang, Hai Su, Xiao-Peng Shen, Peng Zhan, Ming-Hui Lu, Zhen-Lin Wang, and Yan-Feng Chen, “Visualization of higher-order topological insulating phases in two-dimensional dielectric photonic crystals,” *Phys. Rev. Lett.* **122**, 233903 (2019).
- [44] Xiao-Dong Chen, Wei-Min Deng, Fu-Long Shi, Fu-Li Zhao, Min Chen, and Jian-Wen Dong, “Direct observation of corner states in second-order topological photonic crystal slabs,” *Phys. Rev. Lett.* **122**, 233902 (2019).
- [45] Yasutomo Ota, Feng Liu, Ryota Katsumi, Katsuyuki Watanabe, Katsunori Wakabayashi, Yasuhiko Arakawa, and Satoshi Iwamoto, “Photonic crystal nanocavity based on a topological corner state,” *Optica* **6**, 786–789 (2019).
- [46] Haoran Xue, Yahui Yang, Fei Gao, Yidong Chong, and Baile Zhang, “Acoustic higher-order topological insulator on a kagome lattice,” *Nat. Mater.* **18**, 108 (2019).
- [47] Xiujuan Zhang, Hai-Xiao Wang, Zhi-Kang Lin, Yuan Tian, Biye Xie, Ming-Hui Lu, Yan-Feng Chen, and Jian-Hua Jiang, “Second-order topology and multidimensional topological transitions in sonic crystals,” *Nat. Phys.* **15**, 582 (2019).
- [48] Jiho Noh, Wladimir A Benalcazar, Sheng Huang, Matthew J Collins, Kevin P Chen, Taylor L Hughes, and Mikael C Rechtsman, “Topological protection of photonic mid-gap defect modes,” *Nat. Photonics* **12**, 408 (2018).
- [49] Tao Liu, Yu-Ran Zhang, Qing Ai, Zongping Gong, Kohei Kawabata, Masahito Ueda, and Franco Nori, “Second-order topological phases in non-hermitian systems,” *Phys. Rev. Lett.* **122**, 076801 (2019).
- [50] Xiang Ni, Matthew Weiner, Andrea Alù, and Alexander B Khanikaev, “Observation of higher-order topological acoustic states protected by generalized chiral symmetry,” *Nat. Mater.* **18**, 113 (2019).

- [51] Yoshihiro Akahane, Takashi Asano, Bong-Shik Song, and Susumu Noda, “High-q photonic nanocavity in a two-dimensional photonic crystal,” *Nature* **425**, 944–947 (2003).
- [52] Gilbert Strang and George J Fix, *An analysis of the finite element method*, Vol. 212 (Prentice-hall Englewood Cliffs, NJ, 1973).
- [53] J Zak, “Berry’s phase for energy bands in solids,” *Phys. Rev. Lett.* **62**, 2747 (1989).
- [54] Feng Liu and Katsunori Wakabayashi, “Novel topological phase with a zero berry curvature,” *Phys. Rev. Lett.* **118**, 076803 (2017).
- [55] Gunnar Bjork and Yoshihisa Yamamoto, “Analysis of semiconductor microcavity lasers using rate equations,” *IEEE J. Quantum Electron.* **27**, 2386–2396 (1991).